Chemical and Process Engineering: New Frontiers, 2023, 44(4), e38
DOI: 10.24425/cpe.2023.147397

A study of the thermal regeneration of loaded hydrophobic and hydrophilic zeolites after adsorption in the liquid phase

Piotr Tabero[1], Elżbieta Gabruś[2]*

[1] West Pomeranian University of Technology in Szczecin, Faculty of Chemical Technology and Engineering, Department of Inorganic and Analytical Chemistry, Piastów 42, 71-065 Szczecin, Poland
[2] West Pomeranian University of Technology in Szczecin, Faculty of Chemical Technology and Engineering, Department of Chemical and Process Engineering, Piastów 42, 71-065 Szczecin, Poland

*** Corresponding author:**
e-mail:
Elzbieta.Gabrus@zut.edu.pl

Presented at 24th Polish Conference of Chemical and Process Engineering, 13–16 June 2023, Szczecin, Poland.

Article info:
Received: 15 May 2023
Revised: 10 July 2023
Accepted: 31 July 2023

Abstract
The paper aims to show a search method for optimal conditions of 3A, 13X, ZSM-5 zeolite thermal regeneration after adsorption from a liquid water-isopropanol mixture. Comparative TGA-DTG results for heating of wet zeolites with different structure and hydrophobicity showed characteristic effects corresponding to the optimal temperature of zeolite regeneration. The consequences of overheating and collapse of the 3A, 13X, ZSM-5 zeolite structure at temperatures of 850, 900, 1000 °C, respectively, were recorded with XRD method. Moreover, XRD and NIR/DRS tests of loaded and regenerated zeolite samples showed interaction of adsorbate and co-adsorbed water with adsorbent and revealed influence of adsorption and regeneration processes on the adsorbent structure. Investigations of the regeneration of the zeolite 3A bed after adsorption of water from the isopropanol solution in the temperature swing adsorption (TSA) process were carried out by heating the bed with inert gas at 250 °C and different purge gas streams in the range of 1.68–2.40 kg/h. Four stages of wet bed regeneration were distinguished, which corresponded to the effect observed during TGA-DTG tests. For each stage, the specific demand for purge gas and energy was determined depending on the gas stream and its minimum value of 2.16 kg/h was indicated.

Keywords
adsorptive dewatering of liquid, NIR spectroscopy, TGA/DTG, XRD, fixed bed regeneration

1. INTRODUCTION

Adsorption from liquids is a technique for treating waste solution and streams with low pollutant concentrations, most often used for water treatment or liquid dewatering (Bonilla-Petriciolet et al., 2017; Worch, 2012). The liquid streams can be treated in a column installation that operates periodically in adsorption and thermal regeneration in a cyclic process called temperature swing adsorption (TSA). The adsorption stage usually takes place at room temperature on a fixed bed of adsorbent, such as activated carbon or zeolite. Then, the stages of thermal regeneration of the loaded bed and its cooling are carried out, usually combined with the recovery of the adsorbate (Crittenden and Thomas, 1998). Each adsorption system requires individual determination of operating conditions for both adsorption and regeneration, which depend on the adsorbate, adsorbent and their mutual interactions. Carbon adsorbents and zeolites are the most common in adsorption processes (Li et al., 2021). Activated carbons are used for adsorption of organic compounds from the aqueous phase, which are non-selective adsorbents with a wide spectrum of pores, from macropores through mesopores to micropores. They have a greater affinity for organic compounds and are capable of adsorbing molecules of various diameters, and are mainly used in water purification process (Bonilla-Petriciolet et al., 2017; Worch, 2012).

On the other hand, zeolites are considered to be selective adsorbents due to their structure prepared by mixing zeolite crystallites (diameter $\sim$ 1 µm) with clay as a binder in the amount of 16–20%. Adsorbents prepared in this way are porous solids with both macropores and micropores. The macropores in the binder are wetted with a liquid mixture, and the micropores in the zeolite crystallites are capable of selective adsorption of water molecules and other compounds whose size is smaller than narrow structural cages (Gabruś et al., 2015; Prokof'ev et al., 2019). Microporous crystalline aluminosilicates in zeolite are composed of SiO_4 and AlO_4 tetrahedra with O atoms connecting neighboring tetrahedra. As the Si/Al ratio of the framework increases, the zeolite hydrophobicity increases. Low-silica zeolites (such as 3A, 4A, 13X with Si/Al ratios of 1–3) are hydrophilic, whereas high-silica zeolites (such as ZSM-5) are hydrophobic with Si/Al ratios of 10–100 (or higher). Regardless of the tendency to hydrophobicity, each granular zeolite will be saturated in the macroporous structure with a liquid mixture also containing water. Regardless of Si/Al ratio, fresh zeolites contain at least 1–2% of adsorbed water (Hoff et al., 2016).

In many applications, it is necessary to dewater liquids before they can be used in further processes, and this is especially the case with organic liquids. The removal of water from the liquid is aimed at preventing formation of hydrates, catalyst poisoning and corrosion. Liquid drying can be carried out by

distillation, membrane permeation, adsorption and chemical reaction with desiccants such as $CaCl_2$, NaOH (Ambrożek et al., 2013; Joshi and Fair, 1991).

The chemical desiccants are suitable for one-time applications, whereas adsorbent materials can be applied multiple times as they can be regenerated and reused. Adsorption is preferred to remove small amounts of water until it is completely removed from the organic liquid (Ambrożek et al. 2012; 2013). A widely used group of organic liquids are aliphatic alcohols, which are hygroscopic and also form azeotropes with water. One of the most common organic liquids used is isopropyl alcohol (IPA) which is mainly consumed in the electronics and medical device sectors. Moreover, it is also an essential agent used in the processing of essential oils, fats, fragrances, waxes in quick wash extraction, in coatings, automotive and food industries and for manufacturing medicines. IPA is the simplest secondary alcohol that has three carbon atoms in the molecule and a hydroxyl group (-OH) in the middle. Its oxygen has a partial negative charge, while the connecting hydrogen and carbon atoms have partial positive charges, making IPA a polar molecule. Miscible in water, IPA also dissolves a wide range of nonpolar compounds like oils and resins. Isopropyl alcohol is a flammable liquid with an irritating odor and is recognized as a universal solvent, especially in innovative water-sensitive applications (Haider et al., 2021; Luzanova et al., 2023; Nastaj and Aleksandrzak, 2013; Prasakti et al., 2020).

From an economic point of view, the success of the adsorption system application also depends on the possibility of carrying out an effective and low-energy regeneration of the adsorbent. In TSA processes, the method of heat supply may vary, but the temperature of the bed reached during its heating is crucial. In this paper, we consider the case of heating with a stream of hot inert gas. The regeneration temperature should be higher than the boiling point of adsorbate, and the highest one should not damage the adsorbent structure responsible for the adsorption capacity. It is also important to estimate the duration of the steps of the TSA process so that the adsorption takes longer than others.

In the case of biporous zeolites, thermal regeneration is a complex process of releasing adsorbed water molecules and proceeds in three steps. In the first step, loosely bonded water (capillary water) is eliminated. Next, desorption of water occurs from α-type cavities and β-cages. Another problem is interaction between water molecules, water molecules and adsorbate molecules or adsorbent (Carteret, 2009). These effects can be observed in TGA/DTA laboratory tests, but it is only on a large-scale laboratory that their real impact on the time and energy demand of regeneration can be seen (Gabruś et al., 2015; 2022). Therefore, the study undertook further comparative and low-cost regeneration tests on a laboratory scale and high-cost regeneration in the TSA installation. This paper also attempts to explain the role of water co-adsorbed with IPA in the adsorption and regeneration processes on biporous adsorbents differing in hydrophobicity. Measurement techniques such as thermogravimetric analysis (TGA), X-ray diffraction (XRD), diffuse reflection spectroscopy in the near infrared (NIR/DRS) and infrared spectroscopy (IR) were used to obtain valuable information about physical phenomena related to the adsorption and regeneration processes of the loaded zeolite adsorbent. The aims of the here presented work are: (i) determination of the favorable temperature for the regeneration of wet zeolite adsorbents based on the results of thermogravimetric studies (ii) investigation of the thermal stability of selected zeolites, (iii) determination of the effect of the adsorbate on the structural properties of the adsorbent, (iv) elucidation of the relationship between the structure of zeolite channels and multi-stage regeneration of the adsorbent, (v) verification of the applicability of the laboratory research results on the thermal regeneration of zeolites to the analysis of the fixed-bed column process, (vi) determination of the value of the purge air stream ensuring minimum energy demand.

2. EXPERIMENTAL

2.1. Materials

Liquid isopropanol (Sigma Aldrich) and water were used for the adsorption tests. The basic proprieties of adsorbates are shown in Table 1.

Table 1. Properties of used adsorbates.

Property	Isopropanol	Water
Molecular mass, M [kg/kmol]	60.10	18.02
Boiling point, T_b [K]	355.8	373.15
Dipole moment, μ [D]	1.58	1.86
Dielectric constant, ε [–]	18.2	80 Evaporation

Three zeolite adsorbents were selected for investigations i.e. a hydrophobic ZSM-5 with the trade name HiSiv-3000 (UP, USA No 8917-999) and a hydrophilic 3A (Sigma Aldrich No 20858-2) and 13X (Sigma Aldrich No 208647).

Strictly defined crystal structure is a crucial property of zeolites determining their field of application and differentiating them from activated carbons (Fujiyama et al., 2014; IZA-SC, 2017; Khoramzadeh et al., 2019; Pasti at al., 2012). Crystal structure of zeolites is built up of corner shared SiO_4 and AlO_4 tetrahedra (TO_4, T = Al, Si). Substitution of Al^{3+} ions for Si^{4+} ones requires compensation of charge by introducing to the crystal lattice an adequate number of positive ions of Na^+, K^+ or Ca^{2+}. Corner shared tetrahedra form complex structures comprising empty spaces like cages and tunnels of different sizes which are called micropores. Owing to defined crystal structure for each zeolite, theoretical values

of volumes of micropores accessible for water molecule can be calculated. Their values related to the volumes of unit cells of given zeolite and expressed in % enable estimation of their sorption capacity. For used zeolites 13X, 3A and ZSM-5 these values are equal to 27.4%, 21.4% and 9.81%, respectively. In such a case adsorbed volumes of water during experimental tests should be comparable to calculated volume of micropores.

Cages and tunnels are composed of multimember rings called windows through which micropores can be penetrated by different molecules provided that their dimensions are smaller than the size of windows forming cages or tunnels. The diameter of multimembered rings composed of SiO_4/AlO_4 tetrahedra present in the crystal structure of zeolites limits the size of adsorbed substances and is responsible for selectivity of adsorbent. The size of window increases with the increase of the number of ring members. Six membered ring (6R) with dimension of window equal to 2,55Å can be penetrated only by the smallest particles like water (2.6 Å diameter). As the Si/Al ratio of the framework increases, the tendency to adsorb polar molecules like water decreases and zeolite is more and more hydrophobic (Olson et al., 2000). Zeolites 3A and 13X with Si/Al ratios of 1 or 3, respectively, are hydrophilic. On the other hand, high-silica zeolite ZSM-5 with Si/Al ratios of 10–100 or higher is hydrophobic. Regardless of the Si/Al ratio, fresh zeolites (taken just from producer container) contain at least 1–2% of adsorbed water (Hoff et al., 2016).

The properties of zeolites can be modified by mixing them (crystallite diameter $\sim$ 1 μm) with clay as a binder in the amount of 16–20%. Adsorbents prepared in this way are porous solids with both macropores and micropores. The macropores in the binder are wetted with a liquid mixture, and the micropores in the zeolite crystallites are capable of selective adsorption of water molecules and other compounds whose size is smaller than narrow structural cages (Gabruś et al., 2015; Prokof'ev et al., 2019). Regardless of the tendency to hydrophobicity, each granular zeolite will be saturated in the macroporous structure with a liquid mixture also containing water.

Zeolite 3A, the member of LTA group is built up of the sodalite β-cages comprising 4-rings and 6-rings windows. Such β-cages linked through double 4-rings form cubic structures with characteristic 8-membered rings and large cage inside, called α-cavity. The crystal structure of 13X zeolite is also built up of the sodalite β-cages, which this time linked through double 6-rings form cubic faujasite structure (FAU) with 12-membered rings and large cavity inside, corresponding to α-cage in LTA structure. On the other hand, the crystal structure of ZSM-5 zeolites comprises straight and zig-zag (sinusoidal) 10-ring channels intersecting with formation of intersection cavity. Thus, in the case of 3A and 13X zeolites two different sorption sites occur, one in smaller sodalite-type β-cages (6R window of 2,55Å diameter) and another one in α-type cavity in 3A (8R, 4.2Å window) and in similar cavity in 13X, but with larger window (12R ,7.4Å window). This type of zeolites exhibits bifurcation behavior. On the other hand, in ZSM-5 three sites are accessible in straight channels, in sinusoidal channels and in intersections, but with very similar dimensions (10R, 5.5Å window).

Water molecule can form up to four hydrogen bonds, their strength increases with increase of their number formed by selected molecule of water (Carteret, 2009; Luck, 1998). Liquid water can also contain no-hydrogen-bonded, so called free water molecule. With the increase of strength of hydrogen bond produced by its absorption bands in near or middle infrared, shifts towards longer wavelengths (lower wavenumbers).

2.2. Methodology

Research on the efficiency of regeneration of used adsorbents was carried out using thermogravimetric analysis (TGA), near infrared spectroscopy (NIR/DRS) and X-ray diffraction (XRD). The XRD method allows to identify the structure of the adsorbent, to track its changes during the adsorption and desorption process and to determine the range of its thermal stability. The TGA measurements provide information on the mass change during heating or cooling of the adsorbent. It is helpful for determining the temperature range of desorption process and boundary of adsorbent thermal stability. On the other hand, the analysis of DTG curve (the first derivative of mass loss with respect to temperature) enables to estimate the rate of adsorbate desorption and recognize the stages of desorption process. Both spectroscopic methods, IR and NIR/DRS, are useful for detection and identification of the adsorbed molecules in loaded adsorbent and for following their interactions during the adsorption or desorption process.

2.2.1. XRD

Powder diffraction patterns were recorded using Empyrean II diffractometer of PANalytical, The Netherlands, equipped with copper tube, graphite monochromator, and PIXcel^{3}D detector. The identification of phases was performed using the ICDD PDF4 + 2023 database. The analysis of diffraction patterns was performed using Highscore + software and Origin 8 software package (OriginLab, USA).

2.2.2. NIR/DRS

The near infrared spectra (NIR/DRS), were recorded in the wavelength region of 800–2400 nm with 5 nm increment using JASCO-V670 spectrometer (Japan) equipped with an integrating sphere PIN 757. The spectrometer was calibrated using Spectralon. Liquid samples were investigated in a transmission mode in quartz cuvettes of 1 mm thickness.

2.2.3. Thermal analysis

Thermogravimetric examinations (TGA, mass change with increase of temperature) were performed using SDT 2960 apparatus (TA Instruments, USA), (sample mass of around 25 mg, temperature range up to 1000 °C, argon flow rate of 110 ml/ h, corundum crucibles, the heating rate of 10 °C/min.). The TGA curves in digital form were analyzed using the Origin 8 software package (OriginLab, USA).

For desorption tests, approximately 5g samples of fresh adsorbents were gradually flooded with liquid IPA or water in Petri dish until they began to look wet. Next, in the form of original beads, they were subjected to XRD, TGA and NIR/DRS investigations. In indicated in the text cases adsorbent beads were crushed and grinded in a mortar before measurements (Gabruś et al., 2015; 2022).

2.3. Temperature swing adsorption studies

A fixed bed experimental installation is presented in Fig. 1 and was used to investigate isopropyl alcohol dewatering from liquid water-alcohol solution using zeolite molecular sieves 3A and then zeolites regeneration by thermal heating with inert gas at 250 °C. The column diameter was 50 mm, height 760 mm. The column was insulated with 50 mm thickness mineral wool. The cyclic temperature swing adsorption process consisted of two main steps: adsorption from the liquid phase and thermal regeneration with hot gas. The tests of both successive stages were carried out in an experimental installation with a fixed bed on a bench scale (Fig. 1).

The stage of adsorptive removal of water from liquid alcohol was carried out until the zeolite molecular sieve bed was saturated. At the end of adsorption stage, the bed was completely flooded with liquid, and the column inlet and outlet concentrations became equal. The loaded zeolite wet bed in the column was regenerated in stages to restore the bed to a reusable state in the cyclic adsorption process. First, the column was emptied of the water-alcohol feed solution by gravity and additionally the column was briefly blown with a stream of cold air in order to remove the liquid from the surface layer of the adsorbent. The main regeneration consisted in heating the zeolite bed with a stream of hot air and then cooling it with a stream of cold air. The final steps were long. The thermal step of regeneration in the column was carried out by means of a stream of hot air with a constant temperature of 250 °C. The hot gas with the desorbed water-alcohol mixture was directed to the cooler, where the desorbate was condensed, its weight was recorded and its composition was analyzed with chromatography. The flow direction of the hot (or cold) air stream in the regeneration stage is from top to bottom, i.e. opposite to the flow of the liquid mixture in the adsorption stage. As a result of the measurements, concentration curves and temperature profiles were obtained.

3. RESULTS AND DISCUSSION

3.1. Influence of the adsorbate on the diffraction pattern of the adsorbent

In the course of adsorption process, adsorbed molecules affect the structure of adsorbent causing small shifts of atoms building its structure. This, in turn, affects the values of the unit cell parameters and the associated diffraction reflection positions. The shifts of diffraction reflections are relatively small (0.01–0.4 ° 2θ), but measurable by diffraction methods (Fujiyama et al., 2014; Pasti at al., 2012). Diffraction patterns of ZSM-5, 13X and 3A zeolites recorded after adsorption of water were compared to diffractograms of fresh zeolites (Fig. 2). Powder diffraction pattern of ZSM-5 zeolite recorded after adsorption of water with respect of position of diffraction lines and their intensities is very similar to that of fresh ZSM-5 zeolite (Fig. 2A). The only change is a small shift of (1 3 –3)–(1 3 3) pair of reflections which is a stage in the course of polymorphic phase transition from monoclinic to orthorhombic modification of ZSM-5 (Ardit et al., 2015). In the case of 13X and water, irregular changes of diffraction reflection intensities were observed, whereas absorption of water in 3A zeolite was accompanied by increase of intensities of most reflections (Fig. 2C). Despite the small di-

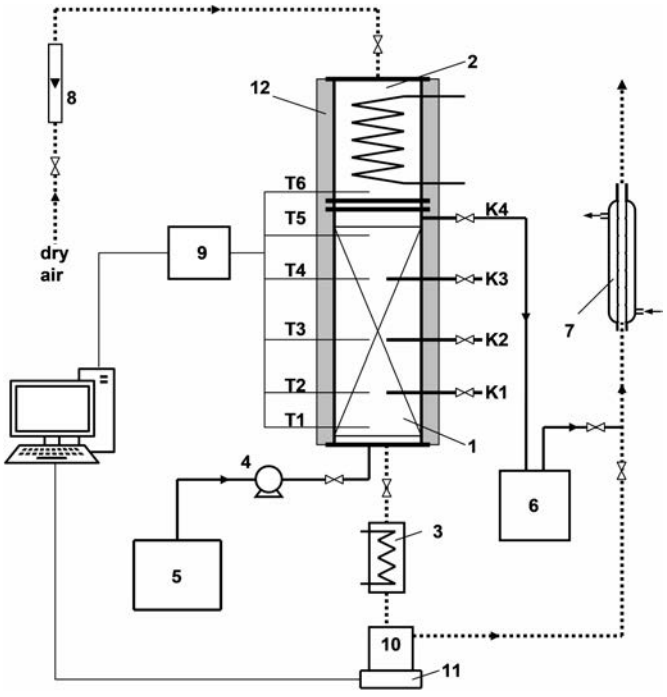

Figure 1. Scheme of the experimental installation: 1 – adsorption column with zeolite fixed bed, 2 – air heater, 3 – vapor condenser, 4 – peristaltic pump, 5 – feed vessel with water-alcohol solution, 6 – dewatered alcohol storage vessel, 7 – reflux condenser, 8 – rotameter, 9 – temperature control system, 10 – water condensed vessel, 11 – electronic balance, 12 – insulation, T – temperature sensor, K – sampling port.

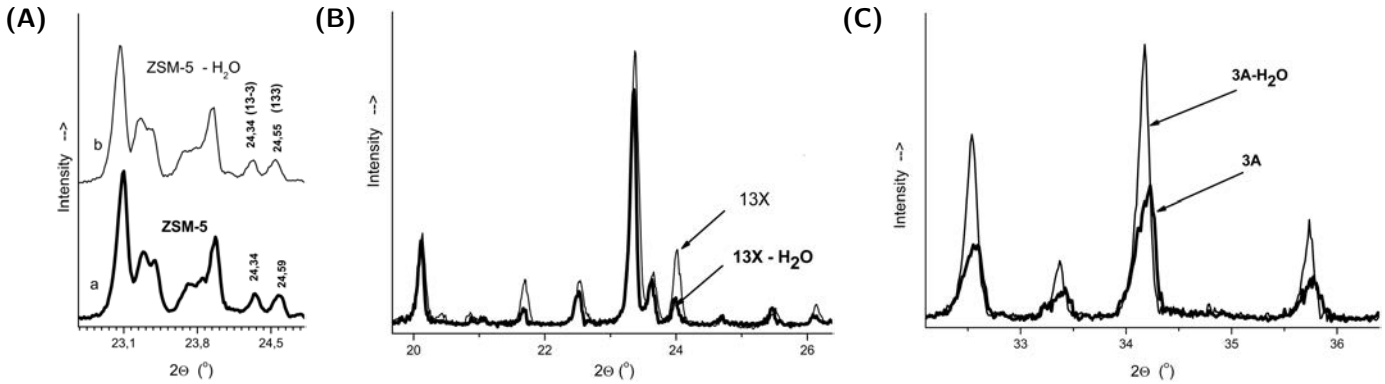

Figure 2. The fragments of powder diffraction patterns showing the changes in powder diffraction patterns characteristic of ZSM-5 (A) 13X (B) and 3A (C) after adsorption of water.

mensions of water molecules, adsorption of water made some impact on the structure of ZSM-5, 13X and 3A zeolites. It is worth noting that after regeneration of the spent adsorbents, the diffraction reflections return to their initial intensities and angular positions recorded on the diffractogram of fresh zeolites. Return of the diffraction reflection after regeneration to starting values seems to corroborate that adsorbate molecules occupy the sorption positions in an ordered way. Thus, conducted tests revealed that small, but measurable changes of positions and intensities of reflections recorded in powder diffraction patterns of zeolites after adsorption or regeneration process can be the indicators of progress of sorption process and corroborate the preservation of zeolitic structure of adsorbent. The analysis of powder diffraction patterns of used in our work zeolites revealed the presence of sharp and intense diffraction reflections characteristic of ZSM-5, 13X and 3A (Fig. 2) corroborating their good crystallinity and defined crystal structure.

3.2. TGA-DTG method for investigation of thermal regeneration of saturated zeolite

The run of the water desorption process from LTA type zeolites was the subject of investigations of (Borthakur and Chattaraj, 1979). According to authors desorption process can be divided into three stages. The first in the temperature boundary of RT-120 °C is connected with elimination of physically adsorbed surface moisture. In the range of 120–400 °C, zeolitic water is eliminated and above 400 °C to 600 °C the same is true of strongly bonded water. On DTG curves of samples the authors recorded two maxima at 120 °C and at 230 °C. On the other hand, Borisova and co-workers (Borisova et al., 2021) studied water desorption from sodalite and LTA zeolites putting emphasis on structure of adsorbents, comprising β cages (sodalite) or β and α cages (LTA). On the DTG curve of sodalite authors recorded two effects with maxima at 95 and 190 °C, attributed to desorption of water from β-cages. In turn on the DTG curve of LTA samples, two effects were recorded with maxima at 50 °C and 150 °C. In both cases the first effect is attributed to desorption of water physically adsorbed from the surface of the particles. In the second stage water is desorbed from α and β cages. With further increase of temperature, strongly bounded water starts to be desorbed.

To get some insights into to process of regeneration of fixed bed from IPA-water mixture, several samples were investigated using TGA-DTG method. In the first stage of test samples of fresh 13X and 3A zeolites and 13X, 3A and ZSM-5 zeolites after adsorption of water were subjected to TGA-DTG investigations (Fig. 3A and 4A. The TGA-DTG tests (Fig. 3A) showed that in accordance with literature data sorption capacity for water increased in the following order: ZSM-5 $<$ 3A $<$ 13X (Khoramzadeh et al., 2019; Milestone and Bibby, 1984). In the case of zeolite 3A, additional TGA tests were performed. Figure 3B shows the recorded TGA curves. After water adsorption, the zeolite sample was regenerated at 500 °C for 1 hour and placed in a tightly closed glass container. Then, one aliquot of the regenerated zeolite granule sample was subjected to TGA (Fig. 3B, curve c). In the next test, a sample of the regenerated zeolite was ground in an air atmosphere in a mortar and tested with the TGA method (Fig. 3B, curve b). The sample after the TGA test was ground in a mortar and subjected to TGA test again (Fig. 3B, curve d). Figure 3B also shows the TGA curve recorded during the regeneration of zeolite 3A after water adsorption (Fig. 3B, curve a). On the TGA curve of a sample of regenerated zeolite ground in a mortar before TGA testing, a significant weight loss was recorded. However, it starts at 160 °C, which corresponds to the end temperature of the first stage of desorption of the used zeolite. This clearly indicates that the β-cages may play a significant role in the initial stage of adsorption of the regenerated adsorbent. On the other hand, the test consisting in double TGA testing up to 1000 °C of the same sample showed that minimal weight loss was registered during the repeated TGA test. It seems that during the first TGA test, after exceeding the temperature of 850 °C, above which the 3A zeolite structure was destroyed and the main product was nepheline, which no

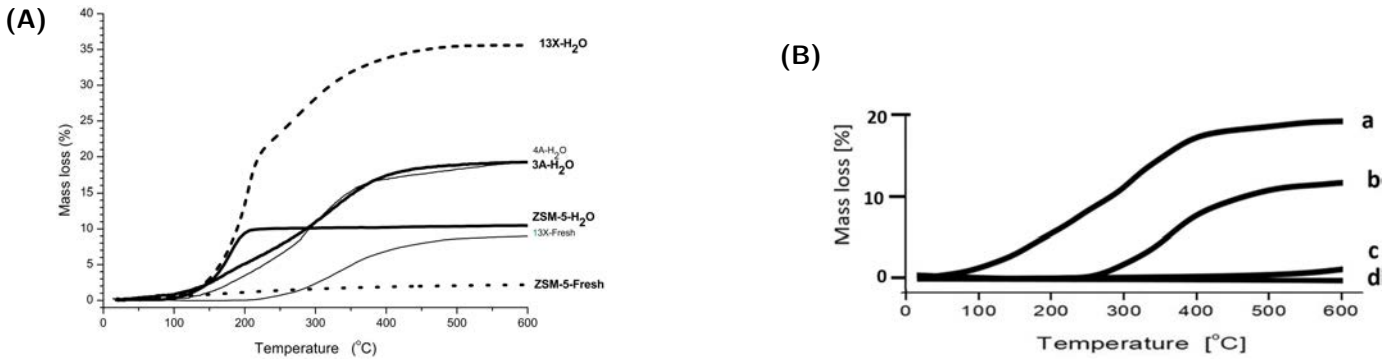

Figure 3. (A) Mass loss curves of fresh 13X and 3A zeolites and 13X, 3A, 4A and ZSM-5 zeolites after adsorption of water, (B) mass loss curves recorded after adsorption of water on 3A zeolite.

longer had adsorption capacity similar to 3A zeolite, despite having practically the same chemical composition.

The analysis of DTG curves (first derivative of mass loss over time) (Fig. 4A) showed that the process of water desorption from ZSM-5 proceeded in one stage, while from zeolites 3A, 4A and 13X it took place in two stages.

The location of the maximum on the DTG curve is also a measure of the bond strength of the adsorbent adsorbate pair. A higher temperature of maximum on the DTG curve indicates a higher binding energy of the adsorbate by the adsorbent.

The analysis of the course of the DTG curves presented in Fig. 4 shows that the first effects (the only effect in the case of ZSM-5) have maxima in a very narrow temperature range of 100–110 °C, and the lowest value, 100 °C, is characteristic of both the hydrophobic zeolite ZSM-5 as well as hydrophilic 3A. For 3A and 13X, maxima of the second effects are in the range of 230–240 °C.

The area under the DTG curve and the intensity of the observed effects are proportional to the amount of mass loss. Analysis of the size of the two effects connected with desorption of water from 3A and 13X zeolites in Figure 4A showed that for zeolites 3A and 4A this relation is 3:4 and for 13X it is 4:1. The analysis of the size of the β and α cages and their number in the unit cell of LTA zeolites showed that their volumes are in relation 1:5. Trying to explain the reason for such a large difference in the size of the effects on the DTG curves, attention should be paid to the fact that the β and α cages are interconnected in a way that allows water molecules to move between them (IZA-SC, 2017; Yanagida et al., 1973). As a consequence, desorption may take place with the participation of water molecules coming from both cages simultaneously.

Analysis of literature data (Borisova et al., 2021) showed that the first step of desorption process is connected with elimination of physically adsorbed surface moisture. As a result of the measurement procedure developed in our laboratory, consisting in drying the granules after water adsorption using paper, the surface layer of the zeolite beads contained only a minimal amount of adsorbate. Under these conditions, measurement results were obtained which not adequately reflected the presence of the surface layer of the adsorbate in comparison with the results presented in the literature. To evaluate this possibility, a series of tests was carried out in which the zeolite granules were not dried using tissue paper. Figure 4B shows the result of such test in the case of adsorption of water by 3A zeolite. Analysis of

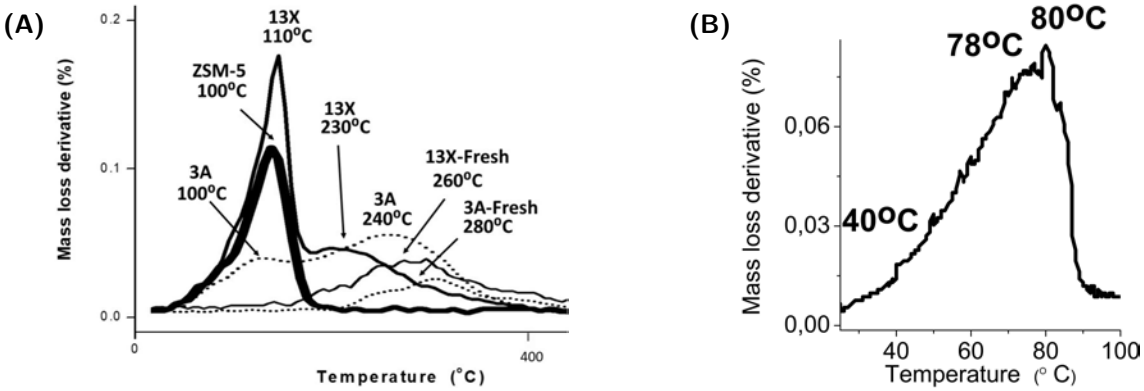

Figure 4. DTG curves recorded during: (A) desorption of water from zeolites 3A, 13X and ZSM-5, (B) for zeolite 3A covered with a thin layer of IPA-water mixture.

the DTG curve in Figure 4B shows a considerable shift of maximum of this curve (78 °C) towards lower temperatures in comparison in 3A curve in Figure 4A (100 °C). Moreover, the recorded curve is asymmetric from the side of lower temperatures suggesting run of the complex desorption process. The analysis revealed also a weak effect at 40 °C and a much better pronounced effect at 82 °C, which can be attributed to the boiling point of IPA.

3.3. Stability of zeolite structure after heating

The knowledge concerning thermal stability of zeolites is of primary importance because their regeneration at too high temperatures leads to collapse of zeolitic structure and to loss of adsorption properties (Gabruś et al., 2015, 2022; Hoff et al., 2016). Producers of zeolites frequently inform customers about the highest safe temperature of its regeneration. In the case of LTA type zeolites (3A) it is approximately 850 °C whereas for FAU zeolites (13X) it is 900 °C. Depending on composition and synthesis procedure ZSM-5 zeolites can decompose in the wide temperature range between 700 °C and 1200 °C (Hoff et al., 2016). In the course of thermal tests, intermediate amorphous phase was identified as well as the drop of intensities of reflection without their broadening or decrease of surface area were observed before cristobalite formation, the end product of ZSM-5 decomposition (Hoff et al., 2016).

In our earlier work it was shown that used by us ZSM-5 zeolite crystallizes in a monoclinic system (PDF card 01-079-7609, formula $Na_{0,03}Al_{0,03}Si_{23,97}O_{48}$) and is stable up to 800 °C (Gabruś et al., 2022). In order to estimate more precisely the temperature of thermal stability several samples of ZSM-5 zeolite were heated at selected temperatures in the range of 900–1200 °C. Figure 5 shows fragments of powder diffractograms of fresh zeolite ZSM-5 (curve a) and sample heated at 1100 °C (curve b). Analysis of recorded diffractograms revealed that ZSM-5 zeolite start to decompose at 1000 °C, what was evidenced by appearance of two weak reflections at 21.58 and 35.70 °2Θ, characteristic of α-cristobalite. The main stage of decomposition takes place in the temperature range of 1000–1100 °C. Powder diffraction pattern recorded after heat treatment at 1100 °C comprised a set of diffraction lines characteristic of α-cristobalite and several weak lines, which can be attributed to α-quartz and ZSM-5 zeolite (Figure 5, curve d). The results of XRD investigations revealed that sample after heat treatment at 1200 °C comprised α-cristobalite with the small admixture of quartz. The lack of diffraction reflections of phases containing silicon and/or aluminium and/or sodium seems to corroborate the low content of aluminium and sodium in the sample of used ZSM-5 zeolite. The results of XRD phase analysis of 13X zeolite sample subjected to TGA investigations up to 1000 °C have shown that product of the decomposition of this sample is nepheline ($Na_{7.15}Al_{7.2}Si_{8.8}O_{32}$, PDF ICDD card 01-0079-0992, general formula $NaAlSiO_4$) with small admixture of quartz (Fig. 5).

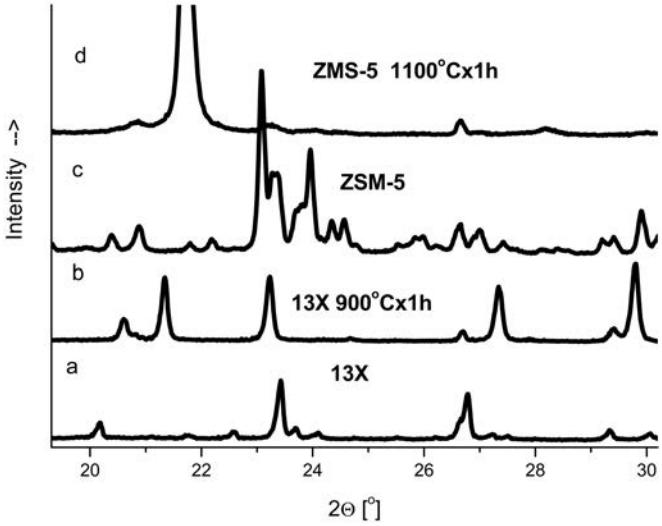

Figure 5. Diffraction patterns of fresh 13X zeolite (curve a) and after heating at 900 °C for one hour (curve b) as well as fresh ZSM-5 zeolite (curve c) and ZSM- zeolite sintered at 1100 °C for one hour (curve d).

Starting 13X zeolite was identified as Na-Faujasite (PDF ICDD card, 04-009-7261 with formula $Na_{15,8}Al_{14}Si_{34}O_{96}$) but its diffraction pattern comprised an additional set of low intensity reflections which were attributed to zeolite binder.

Our current and previous (Gabruś et al., 2015) research reveals that the 3A, 13X, ZSM-5 zeolites structure collapse at temperatures of 850, 900, 1000 °C, respectively.

3.4. NIR method in the study of the adsorption and desorption process

NIR spectrum of water comprises four bands located around 970, 1190, 1450 and 1940 nm (Carteret, 1998; Gabruś et al., 2015; 2022). For analytical purposes in this work were selected two strongest and broadened bands with maxima around 1450 nm (the first overtone of the OH-stretching ($2\nu 1,3$)) and 1940 nm (combination of the OH-stretching band and the O-H bending band ($2n, 3 + n2$) because positions of these bands are affected by the strength and number of hydrogen bonds formed by water molecules (Luck, 1998). On the other hand, NIR band in the range of 1500–1800 nm characteristic of 1–st overtone of C–H stretching vibrations was selected for identification of adsorbates (Beć and Huck 2019; Tomza and Czarnecki, 2015; Wang at al., 2012).

In order to study the relationship between the hydrophobicity of the zeolite and the location of the absorption bands of water adsorbate in the NIR spectrum and to check the possibility of using NIR spectroscopy to study the interactions between adsorbates and the adsorbent several samples were subjected to NIR investigations comprising hydrophobic ZSM-5 and hydrophilic 13X and 3A zeolites as well as water and IPA as the adsorbates. Water with a very small molecule (2.6 Å diameter) can penetrate also β-cages which

will be not accessible for IPA. Thus most of active sites connected with aluminium content in the crystal lattice in the tetrahedral coordination will be accessible for water.

Figure 6A shows three spectra of the hydrophilic zeolite 3A and three spectra of the hydrophobic ZMS-5 zeolite (curves d, e and f) and additionally the spectrum of α-cristobalite (curve g). In turn, Fig. 6B shows the spectrum of fresh 13X (curve d) and zeolite 13X after regeneration at 500 °C for an hour (curve e).

NIR spectrum of hydrophobic fresh ZSM-5 zeolite (Fig. 6A curve d) comprises two broad absorption bands centred at 1400 nm and 1900 nm. The positions of this bands are characteristic of weakly bonded water, so called free water. However, the shoulder at 1457 nm is characteristic for strongly bonded water molecules by one or two hydrogen bonds. On the other hand, positions of these bands in fresh 13X sample were shifted towards higher wavelengths at 1415 and 1914 nm and reaching maximal values 1445 and 1935 nm for 3A. It indicates gradual increase of the strength of hydrogen bonds from ZSM-5 to 3A. The presence in the spectra of these two absorption bands fully proved the content of water in fresh zeolites (Carteret, 2009; Luck, 1998). After regeneration at 500 °C (Fig. 6A curve b and e and Fig. 6B, curve e) both bands were clearly narrowed and their intensities slightly decreased. In the case of the ZSM-5 and 3A samples, the position of the absorption bands did not change. This means that during the regeneration of the zeolite, the water molecules bound with strong bonds were desorbed. In this case, in the spectrum of the regenerated 13X sample, inflections at 1457 and 1975 nm were identified, the presence of which is a characteristic feature of water molecules strongly bound by hydrogen bonding. The third samples in each series were degradation products. The spectra recorded in this case were very similar and contained well-defined but low-intensity absorption bands whose maxima were in the range of 1915–1917 nm. A very faint band at 1415 nm was registered in all spectra. This means that the zeolite samples, which differ significantly in chemical composition, lost their sorption capacity after the degradation of the zeolite structure.

Similarly like in the case of thermogravimetric measurements, samples for NIR investigations were dried with paper prior to investigation. Thus, the research aimed at determining the differences between spectra recorded after drying sample or omitting it. The analysis of the position and intensity of the absorption bands in the dried and undried sample (Figure 6B, curves a and c) showed that the spectrum of the wet sample contained both water and IPA absorption bands, but in the tissue-dried zeolite sample no bands characteristic for IPA were recorded in the spectrum.

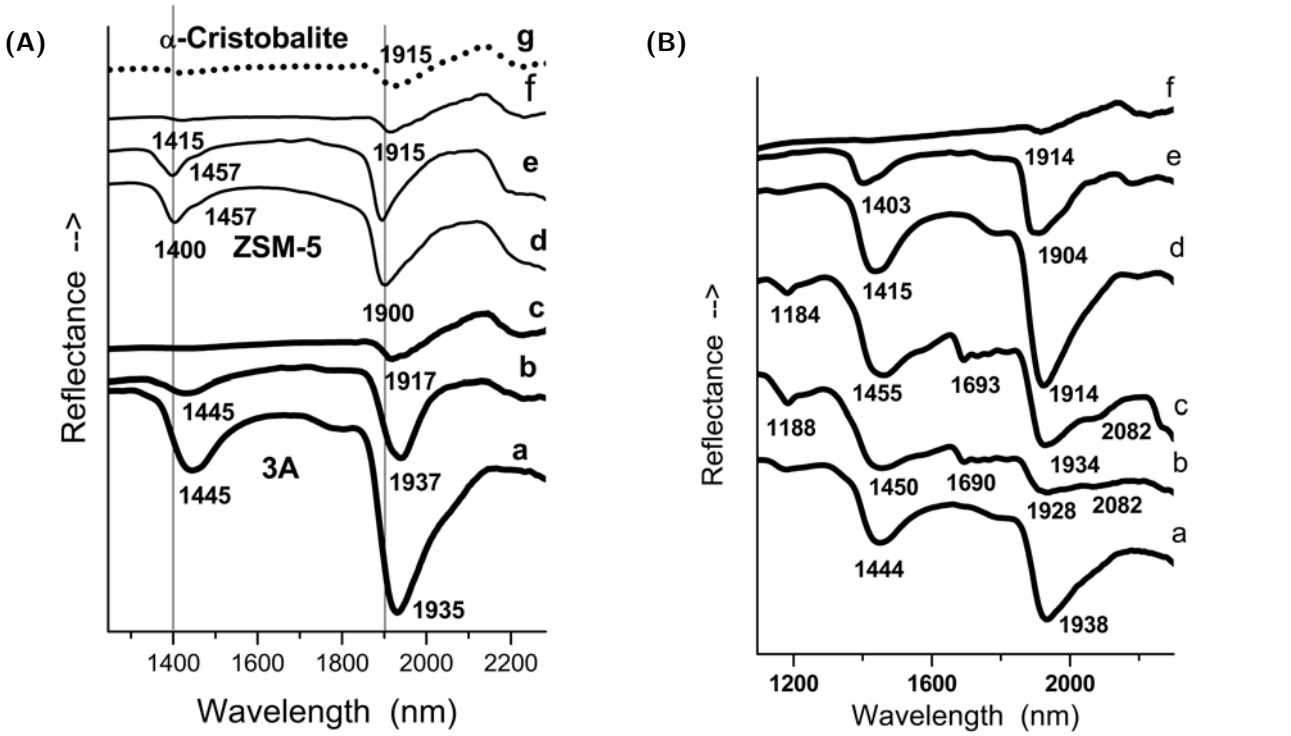

Figure 6. NIR spectra of: (A) fresh 3A zeolite (curve a), 3A after regeneration at 500 °C (curve b), 3A after TGA investigation up to 1000 °C (curve c), fresh ZSM-5 (curve d), ZSM-5 a after regeneration at 500 °C (curve e), ZSM-5 after heating at 1200 °C (curve f) and α-cristobalite (curve g); (B) fresh 13X (curve d), 13X after regeneration at 500 °C (curve e), 13X after TGA investigation up to 1000 °C (curve f), 3A after treatment with the IPA-water mixture (curve c), 3A after treatment with IPA–water mixture, after 10 minutes (curve b) and 3A after treatment with IPA-water mixture and drying with paper before measurement (curve a).

3.5. Stages of thermal regeneration of the zeolite bed

The 3A zeolite bed after the adsorption stage was wet as a result of coming into contact with a liquid mixture of isopropyl alcohol and water. Based on NIR studies (Section 3.4), it is known that hydrophilic zeolite adsorbent 3A selectively adsorbs water molecules, and does not adsorb isopropanol. However, IPA is still present on the bed wetted with the liquid solution. Analysis of the concentration of water and isopropanol at the outlet of the column showed that the concentration of alcohol in the air stream rapidly increased in the initial period to the maximum value, and then decreased to zero before the water concentration increased significantly. In Fig. 7 is clearly visible that the alcohol evaporates first, and then the water. The adsorbent fixed bed can be regenerated by heating method with simultaneous recovery of the adsorbate and to restore the adsorption capacity of the adsorbent bed. In this case, concentrated isopropanol can be recovered, since it is removed from the bed first.

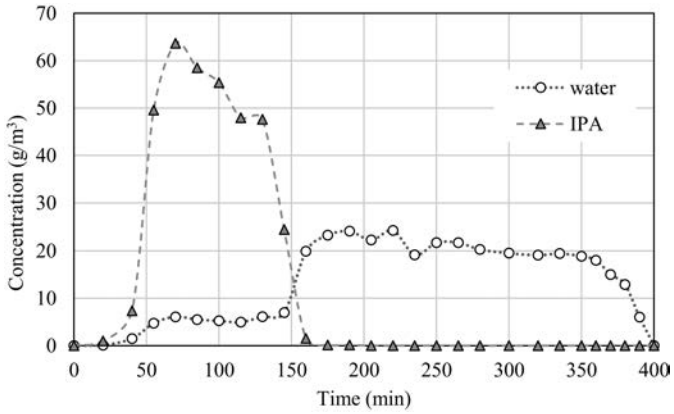

Figure 7. Concentration breakthrough profiles of isopropanol and water vapors at the column (filled 3A zeolite) outlet during thermal desorption step of cyclic TSA process.

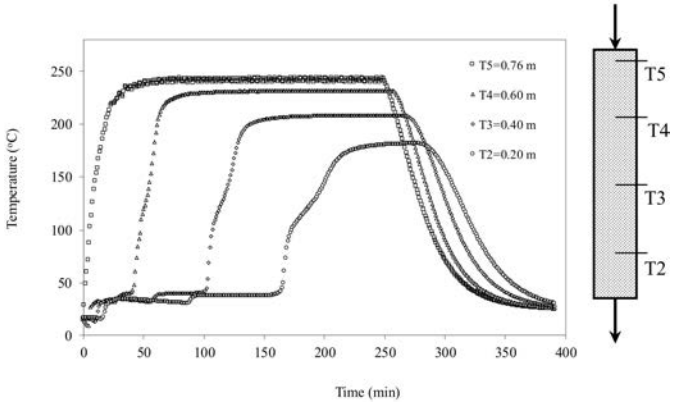

Figure 8. Temperature profiles of 3A zeolite fixed bed at various column positions during isopropanol and water desorption and cooling steps of cyclic TSA process.

During the thermal desorption stage, temperatures at different heights of the bed are monitored (Fig. 8). Temperature profiles have a distinctive course with plateaus and inflection of the curve at specific and repeated temperatures. Initially, the recorded temperature is only 6–7 °C (wet bulb temperature), which corresponds to the removal of the liquid solution from the surface of the wet bed without heating. Then, the temperature is maintained for a long time at about 25 °C and then at about 40 °C, which is observed as two plateaus and corresponds to the removal of liquid from the outer surface of the grains, the binder used in their formation and the macropores of the zeolite. Thereafter, a rapid increase in temperature can be observed until the inflection at 100 °C, when the temperature increase slows down. Another slight upward inflection can be observed at about 125 °C, which can be related to the release of adsorbed water from the micropores. The last inflection of the curve refers to the achievement of a plateau at the temperature resulting from the process conditions and means the end of the release of water from the micropores at a given heating gas temperature. The characteristic areas on the temperature desorption curve correspond to the effects observed at the same temperatures in the TGA studies (Gabruś et al., 2015; 2022).

In adsorption stage, the water molecules in the β and α cages interact with each other by means of hydrogen bonds, the strength of which increases as the number of molecules connected to each other increases. In the process of desorption, the number of water molecules in the adsorbent cages gradually decreases, which leads to the weakening of these interactions.

Analyzing the course of temperature profiles in the light of previous spectroscopic and structural studies (Sections 3.1–3.4), four stages of thermal regeneration of the zeolite bed can be distinguish. The first stage (I) is connected with the evaporation of the liquid from the film wetting the surface of the zeolite grains (about 25 °C). The second stage (II) is related to the evaporation of the liquid from the macropores of the granulated zeolite 3A formed with a binder (bentonite clay) (about 40 °C). The short third (III) stage deals with the desorption of water molecules from the α-cage at about 100 °C. The last fourth (IV) stage is associated with the release of water bound in the micropores of the zeolite in the β-cage structure at a temperature of about 200 °C. As can be seen in Fig. 4, the effects observed during thermal zeolite regeneration on a laboratory scale as local extremes or inflections on the TGA-DTG curves become significant when the process runs on a column scale, where heat transport is accompanied by mass transport.

3.6. Assessment of energy demand during bed regeneration stages

The main operating costs in the TSA process of alcohol dewatering take place in the regeneration stage (Crittenden and Thomas, 1998; Gabruś et al., 2015; 2022). As can be seen

from the conducted research, the desorption of water from hydrophilic zeolites requires a much higher temperature than that of isopropanol evaporation, due to the energy needed to overcome the binding forces of water molecules with the active site inside the zeolite. The methodology of selecting the appropriate temperature for zeolite regeneration is presented in this paper in Section 3.2 in accordance with our previous papers (Gabruś et al., 2015), where the influence of temperature on the demand for inert gas N_p and energy E_p was also examined. These tests are a continuation of the investigations for a constant purge gas temperature at different gas stream values. Column regeneration investigations were performed with a gas inlet temperature of 250 °C and a purge gas stream m_g of 4.67–6.67 · 10^{-4} kg/s. The process parameters are summarized in Table 2, where t_{des} is the desorption time treated as the time of collecting the condensate, m_L is the mass of the IPA solution to be dried, and q_d is the dynamic (working) capacity between the adsorption and regeneration conditions.

Table 2. Selected parameters of process TSA with liquid phase.

No of cycle	$m_g \cdot 10^4$ [kg/s]	t_{des} [s]	m_L [kg]	q_d [$kg_{water}/kg_{zeolite}$]
1	4.67	24000	4.61	0.098
2	5.33	23580	5.21	0.123
3	6.00	21720	5.16	0.125
4	6.67	18720	6.51	0.121

As can be seen in Table 2, the total desorption time t_{des} decreases with the increase in mass flow of purge gas m_g. On the other hand, the dynamic capacity q_d values depend not only on the manner in which the regeneration is carried out, but also on the amount water adsorbed from the organic liquid (m_L) in the adsorption stage of the cyclic TSA process. As can be seen (Table 2), the maximum value of the zeolite 3A bed capacity is 0.125 kg/kg, which is a result comparable to the lowest values achieved on the adsorption of water from alcohols: ethanol, *n*-propanol, *n*-butanol (Gabruś et al., 2015).

The efficiency of the desorption process of both components of the liquid mixture from the fixed bed of the adsorbent depends on the consumption of the purge gas and the demand for energy (Gabruś et al., 2015). In these studies, the presence of four stages of thermal regeneration of the wet bed in the column was taken into account, and for each stage the parameters of purge air and energy demand were determined. These parameters are defined in terms of quantity of purge per amount of adsorbent N_p [kg gas/kg adsorbent], and energy per amount of adsorbent E_p [J/kg adsorbent]:

$$N_p = \frac{m_g \Delta t_i}{m_b} \tag{1}$$

$$E_p = \frac{N_p C_{pg}}{M_g} (T_r - T_0) \tag{2}$$

$$C_{pg} = 31.15 - 1.357 \cdot 10^{-2} T + 2.68 \cdot 10^{-5} T^2 - 1.168 \cdot 10^{-8} T^3 \tag{3}$$

where m_g is mass gas flow in kg/s, Δt_i is duration time of *i*-stage of thermal regeneration (I–IV stages) in s, m_b bed mass in kg, C_{pg} heat capacity of gas in J/(mol·K), M_g is molar mass of gas in kg/kmol and T_0, T_r is a reference and purge gas temperature in K, respectively.

For each thermal regeneration cycle, temperature profiles were obtained at several bed heights and concentration curves at the bed outlet as in Figs. 7 and 8. Based on the column findings, the values necessary to calculate N_p (Eq. 1) and E_p (Eq. 2) were determined. The results of the tests and calculations are shown in Fig. 9.

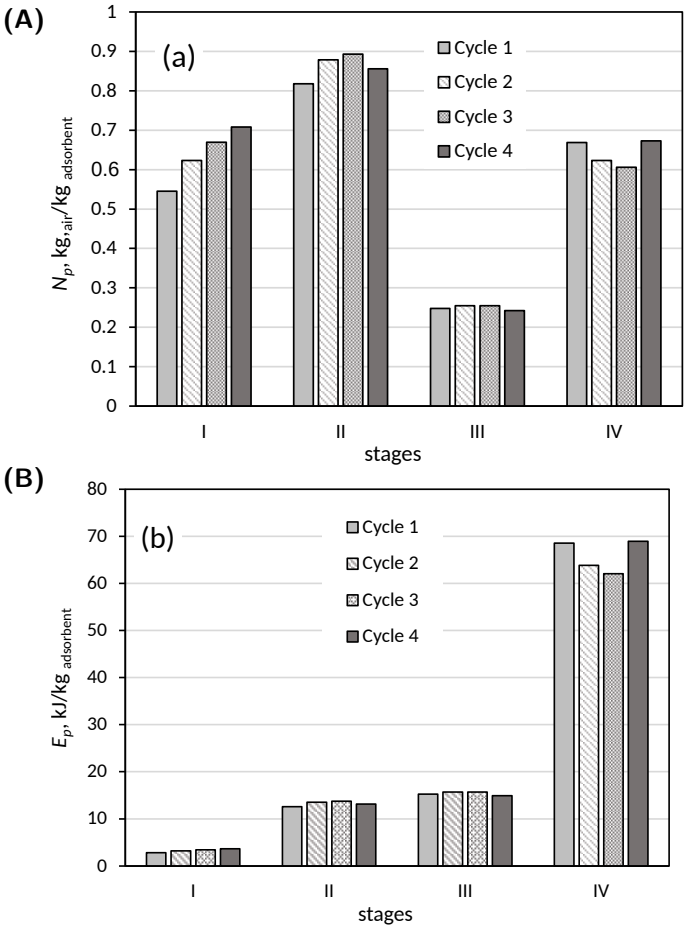

Figure 9. Effect of purge gas stream on specific gas N_p (a) and specific energy E_p (b) consumption.

The purge gas consumption N_p calculated from Equation (1) at various regeneration stages is plotted in Fig. 9A. As can be seen, the highest value is for the longest stage (II) and reaches almost 0.9 kg/kg for cycle 3, and the lowest consumption occurs in the short stage (III) about 0.25 kg/kg. On the other hand, the specific energy consumption E_p de-

termined from Eq. (2) in individual stages has a different tendency. Fig. 9B shows that the highest energy consumption is for stage (IV), but it can also be seen that for the gas mass flow of 0.0006 kg/s, the minimum values of N_p (Fig. 9A) and E_p (Fig. 9B) are achieved. This means that not only the optimal regeneration temperature should be sought, but also the stream of desorbing purge gas should be optimized in order to reduce the costs of the regeneration stage in the TSA process.

4. CONCLUSIONS

The example of water-isopropanol shows the efficiency of adsorptive separation of the liquid mixture with the use of 3A, 13X and ZSM-5 zeolites with different internal structure and hydrophobicity. It was found that based on the knowledge of the internal structure of a given zeolite, it is possible to predict not only the availability and the method of filling the pores of the zeolites, but also the sequence of releasing water and isopropanol molecules in the stage of thermal regeneration of wet zeolite adsorbents.

Analysis of DTG curves showed, that desorption process of water from 3A and 13X zeolites runs in three steps, the first step connected with the release of loosely bonded water is hardly visible in DTG tests. The presence of the second and third steps of desorption in the case of 3A and 13X zeolites and one step in the case of ZSM-5 can be connected with the crystal structure of these adsorbents. The second stage of desorption process of water from 3A, and 13X and the first and the only stage of desorption from ZSM-5 run in almost the same temperature range, which shows that hydrophilic/hydrophobic character of zeolite plays only secondary role in desorption of water from large cages and tunnels characteristic of these zeolites.

The results of the fixed bed regeneration study revealed a multi-stage process of releasing water-containing liquid from the hydrophilic zeolite. The temperatures that characterize these stages correspond to the effects recorded during the thermal analysis, which allows the selection of a favorable temperature for the regeneration of the adsorbent bed. The division of regeneration into stages corresponding to the internal structure of a given zeolite is visible. The conducted analysis of the results of the desorption process tests using the TGA-DTG methods show good agreement with the results of the column tests.

Zeolites exhibit thermal stability over the temperature range used in practical applications in TSA processes. Investigations of thermal stability of 13X and ZSM-5 zeolites revealed that 13X decomposes at about 900 °C with formation of nepheline with a small admixture of quartz, whereas ZSM-5 is stable up to 1000 °C and the product of its decomposition is α-cristobalite with an admixture of quartz.

In the carried out studies of the regeneration of the zeolite 3A bed, the temperature of 250 °C was used, recommended by the results of thermogravimetric tests. Furthermore, column studies have shown that it is possible to find the optimal value of the purge gas stream to achieve minimum energy consumption at a constant regeneration temperature.

REFERENCES

Ambrożek B., Nastaj J., Gabruś E., 2012. Modeling of adsorptive drying of n-propanol. *Drying Technol.*, 30, 1072–1080. DOI: 10.1080/07373937.2012.684084.

Ambrożek B., Nastaj J., Gabruś E., 2013. Modeling and experimental studies of adsorptive dewatering of selected aliphatic alcohols in temperature swing adsorption system. *Drying Technol.*, 31, 1780–1789. DOI: 10.1080/07373937.2013.823442.

Ardit M., Martucci A., Cruciani G., 2015. Monoclinic–orthorhombic phase transition in ZSM5 zeolite: spontaneous strain variation and thermodynamic properties. *J. Phys. Chem. C,* 119, 7351–7359. DOI: 10.1021/acs.jpcc.5b00900.

Beć K.B., Huck C.W., 2019. Breakthrough potential in near-infrared spectroscopy: Spectra simulation. A review of recent developments. *Front. Chem.*, 7, 48. DOI: 10.3389/fchem.2019.00048.

Bonilla-Petriciolet A., Mendoza-Castillo D.I., Reynel-Ávila H.E., 2017. *Adsorption processes for water treatment and purification.* Springer Cham. DOI: 10.1007/978-3-319-58136-1.

Borisova T.N., Gordina N.E., Prokof'ev V.Yu., Afanas'eva E.E., Afineevskii A.V., 2021. Water vapor adsorption/desorption on granulated binder-free low-module zeolites. *E3S Web of Conferences*, 266, 02007. DOI: 10.1051/e3sconf/202126602007.

Borthakur P.C., Chattaraj B.D., 1979. Study of Na-A molecular sieve degeneration by thermal analysis. *J. Therm. Anal.*, 17, 67–72. DOI: 10.1007/BF02156598.

Carteret C., 2009. Mid- and near-infrared study of hydroxyl groups at a silica surface: H-bond effect. *J. Phys. Chem.* C, 113, 13300–13308. DOI: 10.1021/jp9008724.

Crittenden B., Thomas W.J., 1998. *Adsorption technology and design.* Butterworth-Heinemann.

Fujiyama S., Seino S., Kamiya N., Nishi K., Yoza K., Yokomori Y., 2014. Adsorption structures of non-aromatic hydrocarbons on silicalite-1 using the single-crystal X-ray diffraction method. *Phys. Chem. Chem. Phys.*, 16, 15839–15845. DOI: 10.1039/c4cp01860e.

Gabruś E., Nastaj J., Tabero P., Aleksandrzak T., 2015. Experimental studies on 3A and 4A zeolite molecular sieves regeneration in TSA process: Aliphatic alcohols dewatering–water desorption. *Chem. Eng. J.*, 259, 232–242. DOI: 10.1016/j.cej.2014.07.108.

Gabruś E., Tabero P., Aleksandrzak T., 2022. A study of the thermal regeneration of carbon and zeolite adsorbents after adsorption of 1-hexene vapor. *Appl. Therm. Eng.*, 216, 119065. DOI: 10.1016/j.applthermaleng.2022.119065.

Haider M.B., Dwivedi M., Jha D., Kumar R., Sivagnanam B.M., 2021. Azeotropic separation of isopropanol-water using natural hydrophobic deep eutectic solvents. J. *Environ. Chem. Eng.*, 9, 104786. DOI: 10.1016/j.jece.2020.104786.

Hoff T.C., Thilakaratne R., Gardner D.W., Brown R.C., Tessonnier J-P., 2016. Thermal stability of aluminum-rich ZSM-5 zeolites and consequences on aromatization reactions. *J. Phys. Chem. C*, 120, 20103–20113. DOI: 10.1021/acs.jpcc.6b04671.

IZA-SC, 2017. *Database of zeolite structures*. Available at: http://www.iza-structure.org/databases.

Joshi S., Fair J.R., 1991. Adsorptive drying of hydrocarbon liquids. *Ind. Eng. Chem. Res.*, 30, 177–185. DOI: 10.1021/ie00049a026.

Khoramzadeh E., Mofarahi M., Lee Ch.-H., 2019. Equilibrium adsorption study of CO_2 and N_2 on synthesized zeolites 13X, 4A, 5A, and beta. *J. Chem. Eng. Data*, 64, 5648–5664. DOI: 10.1021/acs.jced.9b00690.

Li X., Wang J., Guo Y., Zhu T., Xu W., 2021. Adsorption and desorption characteristics of hydrophobic hierarchical zeolites for the removal of volatile organic compounds. *Chem. Eng. J.*, 411, 128558. DOI: 10.1016/j.cej.2021.128558.

Luck W.A.P., 1998. The importance of cooperativity for the properties of liquid water. *J. Mol. Struct.*, 448, 131–142. DOI: 10.1016/S0022-2860(98)00343-3.

Luzanova V.D, Rozhmanova N.B., Volgin Y.V, Nesterenko P.N., 2023. The use of zeolite 13X as a stationary phase for direct determination of water in organic solvents by high-performance liquid chromatography, *Anal. Chim. Acta*, 1239, 340697. DOI: 10.1016/j.aca.2022.340697.

Milestone N.B., Bibby D.M., 1984. Adsorption of alcohols from aqueous solution by ZSM-5. *J. Chem. Technol. Biotechnol.*, 34, 73–79. DOI: 10.1002/jctb.5040340205.

Nastaj J., Aleksandrzak T., 2013. Adsorption isotherms of water, propan-2-ol, and methylbenzene vapors on grade 03 silica gel, Sorbonorit 4 activated carbon, and HiSiv 3000 zeolite. *J. Chem. Eng. Data*, 58, 2629-2641. DOI: 10.1021/je400517c.

Olson D.H., Haag W.O., Borghard W.S., 2000. Use of water as a probe of zeolitic properties: interaction of water with HZSM-5. *Microporous Mesoporous Mater.*, 35–36, 435–446. DOI: 10.1016/S1387-1811(99)00240-1.

Pasti L., Martucci A., Nassi M., Cavazzini A., Alberti A., Bagatin R., 2012. The role of water in DCE adsorption from aqueous solutions onto hydrophobic zeolites. *Microporous Mesoporous Mater.*, 160, 182–193. DOI: 10.1016/j.micromeso.2012.05.015.

Prasakti L., Hartono M., Jati P.P., Setiaji M.F., Wirawan S.K., Sudibyo H, 2020. Problem solving of isopropyl alcohol – water azeotropic characteristics using packed (natural zeolite) bed adsorber. *ASEAN J. Sci. Technol. Dev.*, 37, 21–27. DOI: 10.29037/ajstd.611.

Prokof'ev V.Y., Gordina N.E., Borisova T.N., Shamanaeva N.V., 2019. Study of the kinetics of water desorption on binder-free pellets of SOD and LTA zeolites using model-free isoconversion analyzes. *Microporous Mesoporous Mater.*, 280, 116–123. DOI: 10.1016/j.micromeso.2019.01.028.

Tomza P., Czarnecki M.A., 2015. Microheterogeneity in binary mixtures of propyl alcohols with water: NIR spectroscopic, two-dimensional correlation and multivariate curve resolution study. *J. Mol. Liq.*, 209, 115–120. DOI: 10.1016/j.molliq.2015.05.033.

Wang X., Bao Y., Liu G., Li G., Lin L., 2012. Study on the best analysis spectral section of NIR to detect alcohol concentration based on SiPLS. *Procedia Eng.*, 29, 2285–2290. DOI: 10.1016/j.proeng.2012.01.302.

Worch E., 2012. *Adsorption technology in water treatment: Fundamentals, processes, and modeling*. De Gruyter, Berlin, Boston. DOI: 10.1515/9783110240238.

Yanagida R.Y., Amaro A.A., Seff K., 1973. Redetermination of the crystal structure of dehydrated zeolite 4A. *J. Phys. Chem.*, 77, 805–809. DOI: 10.1021/j100625a014.